

Towards One Model for Classical Dimensionality Reduction: A Probabilistic Perspective on UMAP and t-SNE

Aditya Ravuri

University of Cambridge

Neil D. Lawrence

University of Cambridge

Abstract

This paper shows that the dimensionality reduction methods, UMAP and t-SNE, can be approximately recast as MAP inference methods corresponding to a generalized Wishart-based model introduced in [Ravuri et al. \(2023\)](#). This interpretation offers deeper theoretical insights into these algorithms, while introducing tools with which similar dimensionality reduction methods can be studied.

1. Introduction

In the realm of single-cell biology and various other domains with complex, high-dimensional data, dimensionality reduction (DR) algorithms are essential tools for uncovering the underlying structure of data. These algorithms, which include very widely-used techniques like t-SNE ([van der Maaten and Hinton, 2008](#)) and UMAP ([McInnes et al., 2020](#)), are especially valuable for visualizing data manifolds, enabling downstream processing, and the discovery of insightful patterns. A deeper comprehension of these algorithms and their theoretical underpinnings is crucial for advancing their applicability, particularly when prior information is available and improving their interpretability. Our work builds on (and aims to unify fully) the ProbDR framework, which interprets classical DR methods through a probabilistic lens to enable the communication of assumptions, integration of prior knowledge and accounting for noise and confounders.

[Ravuri et al. \(2023\)](#) introduced ProbDR as a framework with two main interpretations: UMAP and t-SNE corresponding to inference over an adjacency matrix, and other classical DR algorithms that utilize eigendecomposition of a PSD matrix as inference using a Wishart generative model on the covariance/precision matrix.

In this work, we further simplify the framework, moving away from the variational interpretation and propose that **all algorithms** with ProbDR interpretations (and hence most classical DR methods) can be written as MAP inference algorithms given the model,

$$\mathbf{S}|\mathbf{X} \sim \mathcal{W}^{\{-1\}}(\mathbf{X}\mathbf{X}^T + \epsilon\mathbf{H}K_t(\mathbf{X})\mathbf{H} + \gamma\mathbf{I}, \nu), \quad (1)$$

where $\mathbf{S} \in S_n^+$ is an estimate of a covariance matrix, $\mathbf{X} \in \mathbb{R}^{n,q}$ corresponds to the set of low (q) dimensional latent variables, $\mathbf{H} = \mathbf{I} - \mathbf{1}\mathbf{1}^T/n$ is a centering matrix, and $K_t(\mathbf{X}_i, \mathbf{X}_j) = (1 + \|\mathbf{X}_i - \mathbf{X}_j\|^2)^{-1}$ is the Student-t *kernel*.

We aim to interpret these DR algorithms as MAP inference methods instead of variational methods as studied in [Ravuri et al. \(2023\)](#); [Van Assel et al. \(2022\)](#). This unifies t-SNE and UMAP-like algorithms with the other algorithms and provides semantic interpretation to UMAP and t-SNE. Additionally, we hope that the tools introduced in this paper will provide researchers with more machinery to understand the behaviour of latent variable models.

2. Background

The ProbDR framework showed that many classical DR algorithms can be expressed as inference algorithms corresponding to a probabilistic model. Algorithms that set the embedding of a high-dimensional dataset $\mathbf{Y} \in \mathbb{R}^{n,d}$ in terms of the eigenvectors of a positive-semi-definite matrix were shown in [Ravuri et al. \(2023\)](#) to correspond to a two-step inference process, where,

1. one first estimates a covariance matrix $\mathbf{S}(\mathbf{Y})$ or a precision matrix $\mathbf{\Gamma}(\mathbf{Y})$ (which a graph Laplacian \mathbf{L} can be an estimate of),
2. then estimates the embedding via maximum a-posteriori given one of the two following models,

$$\begin{aligned} \mathbf{S}|\mathbf{X} &\sim \mathcal{W}(\mathbf{X}\mathbf{X}^T + \sigma^2\mathbf{I}_n, d) \text{ or,} \\ \mathbf{\Gamma}|\mathbf{X} &\sim \mathcal{W}((\mathbf{X}\mathbf{X}^T + \beta\mathbf{I}_n)^{-1}, d). \end{aligned}$$

PCoA, for example, is recovered using the first of these formulations with $\mathbf{S} \equiv \mathbf{Y}\mathbf{Y}^T$. Setting $\epsilon = 0$ in Equation (1) recovers these results.

In the case of UMAP and t-SNE, ProbDR did not specify a generative model for either the data or the covariance but only a generative model for the adjacency matrices that describe the nearest neighbour graph.

Specifically, ProbDR showed that the generative models corresponding to UMAP and t-SNE can be seen as models for adjacency matrices \mathbf{A}' ,

$$p(\mathbf{A}'|\mathbf{X}) = \begin{cases} \text{Categorical}(\text{vec}(\mathbf{A}')|w_{ij}^t(\mathbf{X})) & \text{t-SNE} \\ \prod_{i>j}^n \text{Bernoulli}(\mathbf{A}'_{ij}|w_{ij}^U(\mathbf{X}_i, \mathbf{X}_j)) & \text{UMAP} \end{cases} \quad (2)$$

where,

$$w_{ij}^t = \frac{(1 + \|\mathbf{X}_i - \mathbf{X}_j\|^2)^{-1}}{\sum_{k \neq l} (1 + \|\mathbf{X}_k - \mathbf{X}_l\|^2)^{-1}}, \text{ and } w_{ij}^U = \frac{1}{1 + \|\mathbf{X}_i - \mathbf{X}_j\|^2}.$$

The inference can be done as maximum a-posteriori estimation for \mathbf{X} , given the binary, empirical, nearest-neighbour adjacency matrix $\mathbf{A}'(\mathbf{Y})_{ij} = \mathcal{I}(j \in N(i))$, where $N(i)$ represents the set of nearest neighbours of data point \mathbf{Y}_i . UMAP and t-SNE are typically interpreted in a variational way, however the inference trivially becomes MAP inference when we use $\mathbf{A}'(\mathbf{Y})$ as the variational data-dependent distribution (due to the [Ravuri et al. \(2023\)](#), Appendix B.7, Lemma 13). This interpretation is also presented in [Damrich et al. \(2022\)](#).

This simplification is reasonable due to the findings of [Damrich and Hamprecht \(2021\)](#), where it was found that the relatively complex calculation of the variational probabilities in t-SNE and UMAP can be replaced with simply the adjacency matrices without loss of performance. Our initial experiments also closely aligned with these findings.

Crucially, however, [Becht et al. \(2019\)](#); [Damrich et al. \(2022\)](#) note that the optimisation process is equally as important. As part of an extensive study on the nature of the t-SNE and UMAP loss functions, [Damrich et al. \(2022\)](#) then show how the stochastic optimisation of t-SNE and UMAP can be interpreted to be contrastive estimation with the loss

$$\mathcal{L}(\mathbf{X}) \propto -\mathbb{E}_{ij \sim p} \log \left(\frac{w_{ij}(\mathbf{X})}{w_{ij}(\mathbf{X}) + 1} \right) - m \mathbb{E}_{ij \sim \xi} \log \left(1 - \frac{w_{ij}(\mathbf{X})}{w_{ij}(\mathbf{X}) + 1} \right), \quad (3)$$

where p represents a discrete distribution that is uniform across the nearest neighbour pairs and zero everywhere else. Similarly, ξ represents a uniform distribution over non-neighbours. m (set to $2n_-$) is a multiplicative hyperparameter proportional to the number of contrastive negatives that affects the strength of repulsion. In [Damrich et al. \(2022\)](#), $w_{ij}(\mathbf{X}) = \frac{1}{\|\mathbf{X}_i - \mathbf{X}_j\|^2}$ recovers UMAP. This bound is important, as we found that a naive optimisation of the Bernoulli likelihood in Equation (2) leads to a poor embedding (although Appendix B offers more commentary on this bound as a Bernoulli likelihood and provides more evidence for our claims).

For this work, we aim to work with such a contrastive loss function and interpret it as a likelihood, but over the latents \mathbf{X} . This is because we were particularly inspired by [Nakamura et al. \(2023\)](#), who showed that contrastive learning methods could be seen as variational algorithms (hence suggesting a link between t-SNE and contrastive learning) and by [Gutmann and Hyvärinen \(2010\)](#), which shows that contrastive losses are estimators of negative log-likelihoods. [Damrich et al. \(2022\)](#) also greatly simplify the UMAP optimisation process.

3. Discussion

This section argues that inference with the generative model in Equation (1) approximately recovers UMAP and t-SNE-like algorithms.

3.1. The proposed model

We first consider MAP inference for \mathbf{X} given the model,

$$\begin{aligned} \nu \mathbf{L} | \mathbf{X} &\sim \mathcal{W}((-\alpha \mathbf{H} \mathbf{D}' \mathbf{H} + \gamma \mathbf{I})^{-1}, \nu), \\ \mathbf{X} &\sim \text{Uniform}(-\infty, \infty), \end{aligned} \quad (4)$$

where \mathbf{D}' is a squared distance matrix, with elements $\mathbf{D}'_{ij} = \log(1 + \|\mathbf{X}_i - \mathbf{X}_j\|^2)$. Let $\mathbf{M} = -\mathbf{H} \mathbf{D}' \mathbf{H}$. \mathbf{M} is PSD (with some interesting properties relating to isometric Euclidean embeddings, see Appendix A.2). The graph Laplacian is computed as $\mathbf{L} = (\mathbf{D} - \mathbf{A})/\bar{d}$, with \bar{d} being the average degree¹. The adjacency matrix $\mathbf{A}_{ij} = 1$ if $p(ij)$ (of Equation (3)) > 0 .

Then, the log-likelihood given the model in Equation (4) is as follows (we focus on just the data-dependent term),

$$\begin{aligned} \log p(\mathbf{X} | \mathbf{L}) &= -0.5\nu \text{tr}(\mathbf{L}(\alpha \mathbf{M} + \gamma \mathbf{I})) + 0.5\nu \log \det(\alpha \mathbf{M} + \gamma \mathbf{I}) + c \\ &\propto -\alpha \text{tr}(\mathbf{L} \mathbf{M}) + \log \det(\alpha \mathbf{M} + \gamma \mathbf{I}) + k \\ &= \alpha \text{tr}(\mathbf{L} \mathbf{H} \mathbf{D}' \mathbf{H}) + \log \det(\alpha \mathbf{M} + \gamma \mathbf{I}) + k \\ &= \alpha \text{tr}(\mathbf{L} \mathbf{D}') + \log \det(\alpha \mathbf{M} + \gamma \mathbf{I}) + k \quad (\text{trace cyclic and } \mathbf{L} \text{ centered}) \\ &= -\alpha \text{tr}(\mathbf{A} \mathbf{D}') + \log \det(\alpha \mathbf{M} + \gamma \mathbf{I}) + k \quad \text{tr}(\mathbf{D}') = 0 \\ &= -\alpha \sum_i \mathbf{A}_i^T \mathbf{D}'_i + \log \det(\alpha \mathbf{M} + \gamma \mathbf{I}) + k \\ &= -\alpha \sum_i \sum_j a_{ij} \log(1 + \|\mathbf{X}_i - \mathbf{X}_j\|^2) + \log \det(\alpha \mathbf{M} + \gamma \mathbf{I}) + k \end{aligned}$$

1. So that its inverse (i.e. the covariance) has diagonal elements around one.

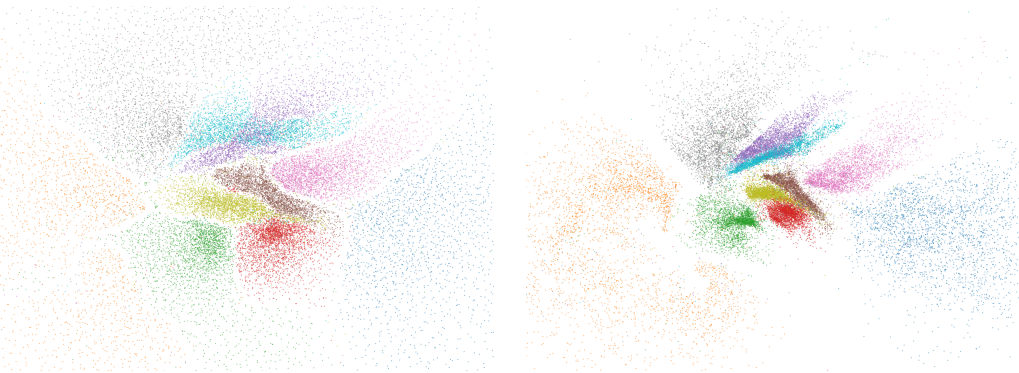


Figure 1: Embeddings of 30k MNIST digits obtained using inference within Equation (4). **Left:** A run with both $\alpha = 1/50$ and $\gamma = 1/5$ treated as hyper-parameters. **Right:** A run with $\alpha = 1/50$ treated as a hyperparameter and γ optimised using maximum likelihood inference. Appendix B sheds light into why this choice of hyper-parameters is performant, leading to the embedding of Figure 4.

$$\begin{aligned}
 &= \alpha \frac{n_+}{\bar{d}} \mathbb{E}_{ij \sim p} \log \left(\frac{1}{1 + \|\mathbf{X}_i - \mathbf{X}_j\|^2} \right) + \log \det(\alpha \mathbf{M} + \gamma \mathbf{I}) + k \\
 &= \alpha n \mathbb{E}_{ij \sim p} \log \left(\frac{w_{ij}(\mathbf{X}_i, \mathbf{X}_j)}{1 + w_{ij}(\mathbf{X}_i, \mathbf{X}_j)} \right) + \log \det(\alpha \mathbf{M} + \gamma \mathbf{I}) + k,
 \end{aligned}$$

with $n_+ = n\bar{d} \approx 1.5nn_{\#}$ being the number of total number of edges and $n_{\#}$ is the number of neighbours per point (typically set to 15). An important note here is that **the model is misspecified** (for example, the variance implied by the covariance parameter and the data are quite different, with the variance of the Wishart being much lower than the data estimate).

Therefore, by minimising the first term of Equation (3), we maximise the data-dependent term of the likelihood of Equation (4), and so, Equation (4) defines a model for dimensionality reduction that in some ways is similar to t-SNE and UMAP-like algorithms. Figure 1 shows embeddings of 30,000 digits from the MNIST dataset obtained using this model. We also run this model on a suite of other datasets (from Pedregosa et al. (2011); Deng (2012); sta; Krumsiek et al. (2011)) to show that we recover roughly similar embeddings as minimisation of Equation (3) in Figure 2.

3.2. CNE bounds can sometimes be approximated using the proposed model

Consider the negative CNE loss,

$$\begin{aligned}
 -\mathcal{L} &\propto \frac{\alpha \nu n}{2} \mathbb{E}_{ij \sim p} \log \left(\frac{w_{ij}(\mathbf{X})}{w_{ij}(\mathbf{X}) + 1} \right) + \frac{\alpha \nu n}{2} m \mathbb{E}_{ij \sim \xi} \log \left(1 - \frac{w_{ij}(\mathbf{X})}{w_{ij}(\mathbf{X}) + 1} \right) \\
 &= -\frac{\nu}{2} \text{tr}(\mathbf{L}(\alpha \mathbf{M} + \gamma \mathbf{I})) + \frac{\alpha \nu n}{2} m \mathbb{E}_{ij \sim \xi} \log \left(\frac{\|\mathbf{X}_i - \mathbf{X}_j\|^2}{1 + \|\mathbf{X}_i - \mathbf{X}_j\|^2} \right) \quad \text{Sec. 3.1}
 \end{aligned}$$

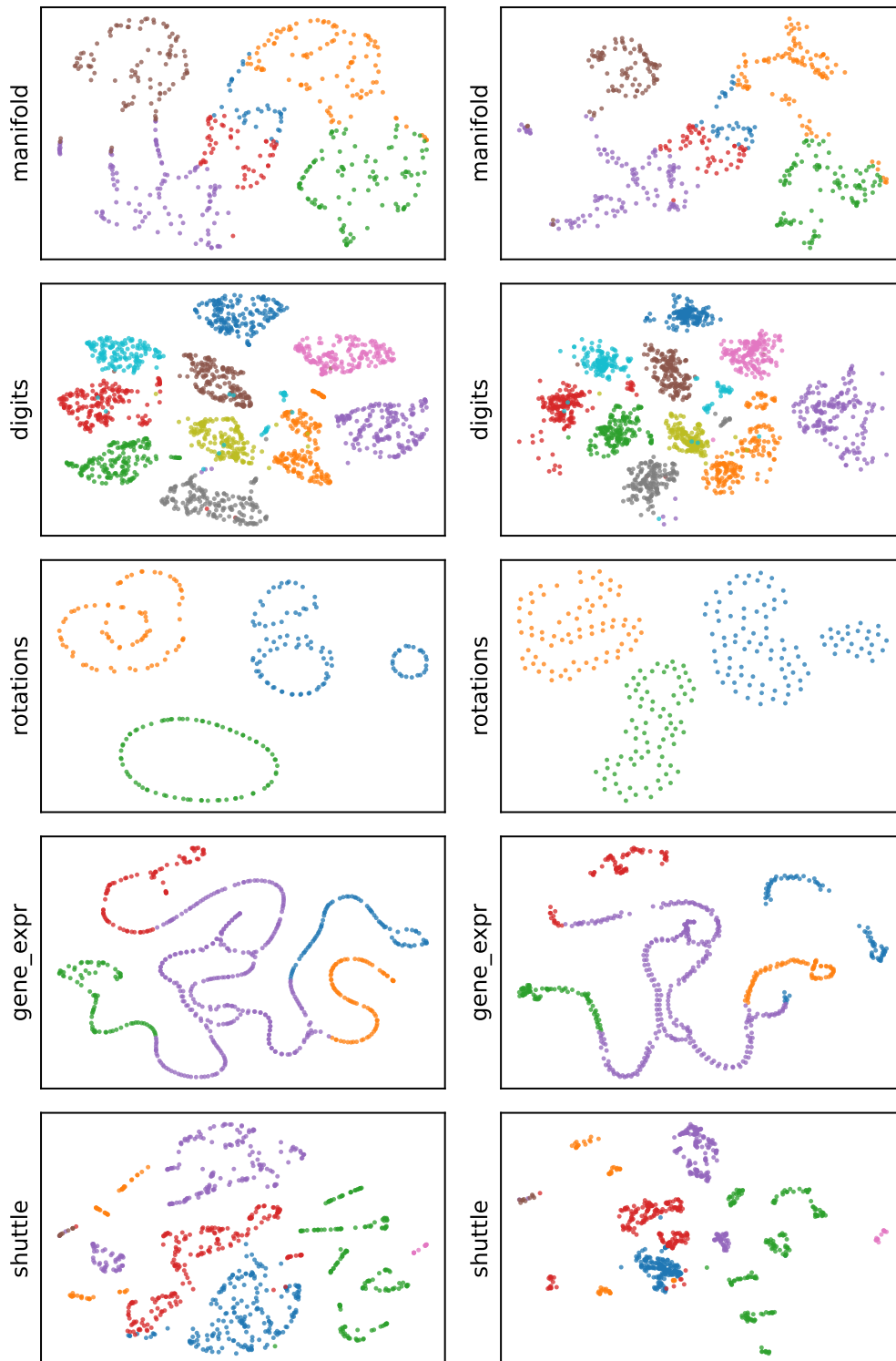


Figure 2: **Left:** embeddings on various datasets obtained using optimisation of the CNE bound (Equation (3)) compared with **right:** inference results using our model.

Let the first term be represented as \mathcal{T}_a . We first approximate the distances $\mathbf{D}'_{ij} = \log(1 + d_{ij}^2) \approx 0.5(1 + d_{ij}^2 - 1/(1 + d_{ij}^2))$ within \mathcal{T}_a as this is a good approximation for the log1p function near 0. Therefore,

$$\mathbf{M} \approx -\mathbf{H}(\mathbf{1}\mathbf{1}^T + 0.5\mathbf{D}^2 - 0.5K_t)\mathbf{H} = \mathbf{X}\mathbf{X}^T + \mathbf{H}K_t\mathbf{H}. \quad \text{App. A.1}$$

This approximation sheds light on the behaviour of the covariance parameter of Equation (4) and draws the link to Equation (1).

Then,

$$\begin{aligned} -\mathcal{L} &\propto \mathcal{T}_a + \frac{\alpha\nu n}{2} m \mathbb{E}_{ij \sim \xi} \log \left(\frac{\|\mathbf{X}_i - \mathbf{X}_j\|^2}{1 + \|\mathbf{X}_i - \mathbf{X}_j\|^2} \right) \\ &\approx \mathcal{T}_a - \frac{\alpha\nu mn}{2} \mathbb{E}_{ij \sim \xi} \left(\frac{1}{1 + \|\mathbf{X}_i - \mathbf{X}_j\|^2} \right) \quad (\text{for large distances}) \\ &\approx \mathcal{T}_a - \frac{\alpha\nu mn}{2} \mathbb{E}_{ij \sim \mathcal{U}} \left(\frac{1}{1 + \|\mathbf{X}_i - \mathbf{X}_j\|^2} \right) \quad \text{as } n \gg n_{\#} \\ &= \mathcal{T}_a - \frac{\alpha\nu mn}{2n^2} \sum_{ij} \frac{1}{1 + \|\mathbf{X}_i - \mathbf{X}_j\|^2} \\ &= \mathcal{T}_a + \frac{\alpha\nu m}{2} \text{tr} \left(-\frac{1}{n} \mathbf{1}\mathbf{1}^T K_t - \frac{1}{n} K_t \mathbf{1}\mathbf{1}^T + \frac{1}{n^2} \mathbf{1}\mathbf{1}^T K_t \mathbf{1}\mathbf{1}^T \right) \\ &= \mathcal{T}_a + \frac{\nu m}{2} \text{tr} (\alpha \mathbf{H} K_t \mathbf{H}) + k \\ &= -\frac{\nu}{2} \text{tr} (\mathbf{L} (\alpha \mathbf{M}_{\text{aprx}} + \gamma \mathbf{I})) + \frac{\nu}{2} \text{tr} (\alpha m \mathbf{M}_{\text{aprx}} + \gamma m \mathbf{I}) - \frac{\alpha m \nu}{2} \text{tr} (\mathbf{X}\mathbf{X}^T) + k \\ &\propto -\frac{m\nu}{2} \text{tr} (m^{-1} \mathbf{L} (\frac{\alpha}{\gamma} \mathbf{M}_{\text{aprx}} + \mathbf{I})) + \frac{m\nu}{2} \text{tr} \left(\frac{\alpha}{\gamma} \mathbf{M}_{\text{aprx}} + \mathbf{I} \right) - \frac{\alpha m \nu}{2\gamma} \text{tr} (\mathbf{X}\mathbf{X}^T) + k \\ &\approx -\frac{m\nu}{2} \text{tr} (m^{-1} \mathbf{L} (\frac{\alpha}{\gamma} \mathbf{M}_{\text{aprx}} + \mathbf{I})) + \frac{m\nu}{2} \log \det \left(\frac{\alpha}{\gamma} \mathbf{M}_{\text{aprx}} + \mathbf{I} \right) - \frac{\alpha m \nu}{2\gamma} \text{tr} (\mathbf{X}\mathbf{X}^T) + k \quad (\text{large } \gamma) \\ &= \log \mathcal{W}(\nu \mathbf{L} | m^{-1} (\alpha \mathbf{M}_{\text{aprx}} + \gamma \mathbf{I})^{-1}, m\nu) + \log \mathcal{N}(\mathbf{X} | \mathbf{0}, \gamma \mathbf{I} / \alpha m \nu) \end{aligned}$$

This shows the NCE bound can be approximated by the likelihood of our proposed model with a diffuse prior on \mathbf{X} . Note that the model is still misspecified. A comparison of embeddings used with this approximation and the CNE bound are shown in Figure 3.

4. Conclusion

We present a probabilistic interpretation of t-SNE and UMAP-like algorithms, showing that they correspond to inference within misspecified generative models for the covariance/precision with fixed scale parameters, and a choice of a covariance that describes non-linear functions within a Gaussian process context. We hope that this serves as a foundation to further refine these models (particularly based on their regularisation terms) such that they emulate results from t-SNE and UMAP-like algorithms.

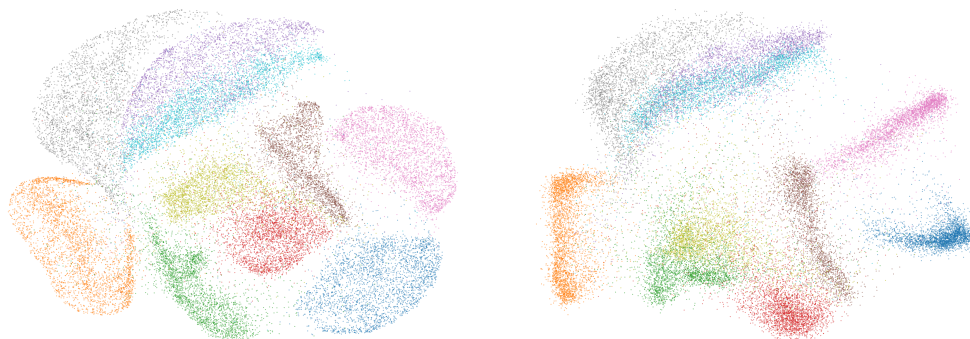


Figure 3: **Left:** Embedding of 30k digits from MNIST obtained using the CNE bound and **right:** using our approximation. For this, we set $n_- = 1$, which was the best performing case.

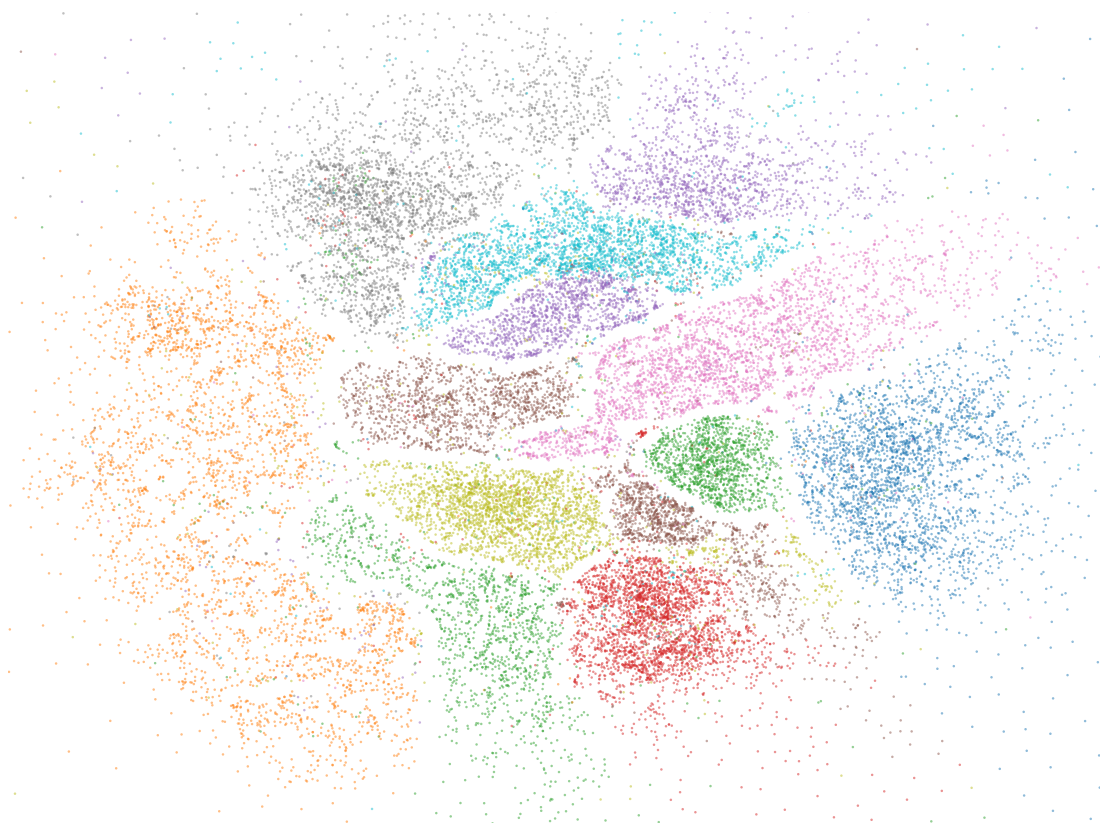


Figure 4: Embedding of 30k MNIST digits resulting from ProbDR inference using a scaled Student-t kernel. See Appendix B.

Acknowledgments

AR would like to thank Francisco Vargas for helpful discussions and a studentship from the Accelerate Programme for Scientific Discovery.

REFERENCES

- Statlog (Shuttle). UCI Machine Learning Repository. URL <https://doi.org/10.24432/C5WS31>.
- Etienne Becht, Leland McInnes, John Healy, Charles-Antoine Dutertre, Immanuel W. H. Kwok, Lai Guan Ng, Florent Ginhoux, and Evan W. Newell. Dimensionality reduction for visualizing single-cell data using UMAP. *Nature Biotechnology*, 37(1):38–44, Jan 2019. ISSN 1546-1696. doi: 10.1038/nbt.4314. URL <https://doi.org/10.1038/nbt.4314>.
- Rajendra Bhatia. *Positive Definite Matrices*. Princeton University Press, 2007. ISBN 9780691129181. URL <http://www.jstor.org/stable/j.ctt7rxv2>.
- Sebastian Damrich and Fred A Hamprecht. On umap's true loss function. In M. Ranzato, A. Beygelzimer, Y. Dauphin, P.S. Liang, and J. Wortman Vaughan, editors, *Advances in Neural Information Processing Systems*, volume 34, pages 5798–5809. Curran Associates, Inc., 2021. URL https://proceedings.neurips.cc/paper_files/paper/2021/file/2de5d16682c3c35007e4e92982f1a2ba-Paper.pdf.
- Sebastian Damrich, Niklas Böhm, Fred A Hamprecht, and Dmitry Kobak. From *t*-sne to umap with contrastive learning. In *The Eleventh International Conference on Learning Representations*, 2022.
- Li Deng. The mnist database of handwritten digit images for machine learning research [best of the web]. *IEEE Signal Processing Magazine*, 29(6):141–142, 2012. doi: 10.1109/MSP.2012.2211477.
- Arjun K Gupta and Daya K Nagar. *Matrix variate distributions*. Chapman and Hall/CRC, 2018.
- Michael Gutmann and Aapo Hyvärinen. Noise-contrastive estimation: A new estimation principle for unnormalized statistical models. In *Proceedings of the thirteenth international conference on artificial intelligence and statistics*, pages 297–304. JMLR Workshop and Conference Proceedings, 2010.
- Apoorva Khare. Schoenberg: from metric geometry to matrix positivity, Apr 2019. URL <https://math.iisc.ac.in/seminar-slides/2019/2019-04-12-ApoorvaKhare.pdf>.
- Jan Krumsiek, Carsten Marr, Timm Schroeder, and Fabian J Theis. Hierarchical differentiation of myeloid progenitors is encoded in the transcription factor network. *PLoS One*, 6(8):e22649, August 2011.
- Leland McInnes, John Healy, and James Melville. UMAP: Uniform manifold approximation and projection for dimension reduction, 2020.

- Hiroki Nakamura, Masashi Okada, and Tadahiro Taniguchi. Representation uncertainty in self-supervised learning as variational inference. In *Proceedings of the IEEE/CVF International Conference on Computer Vision*, pages 16484–16493, 2023.
- F. Pedregosa, G. Varoquaux, A. Gramfort, V. Michel, B. Thirion, O. Grisel, M. Blondel, P. Prettenhofer, R. Weiss, V. Dubourg, J. Vanderplas, A. Passos, D. Cournapeau, M. Brucher, M. Perrot, and E. Duchesnay. Scikit-learn: Machine learning in Python. *Journal of Machine Learning Research*, 12:2825–2830, 2011.
- Aditya Ravuri, Francisco Vargas, Vidhi Lalchand, and Neil D Lawrence. Dimensionality reduction as probabilistic inference. In *Fifth Symposium on Advances in Approximate Bayesian Inference*, 2023. URL <https://arxiv.org/pdf/2304.07658.pdf>.
- I. J. Schoenberg. Remarks to maurice frechet’s article “sur la definition axiomatique d’une classe d’espace distances vectoriellement applicable sur l’espace de hilbert. *Annals of Mathematics*, 36(3):724–732, 1935. ISSN 0003486X. URL <http://www.jstor.org/stable/1968654>.
- Hugues Van Assel, Thibault Espinasse, Julien Chiquet, and Franck Picard. A probabilistic graph coupling view of dimension reduction. *Advances in Neural Information Processing Systems*, 35:10696–10708, 2022.
- Laurens van der Maaten and Geoffrey Hinton. Visualizing data using t-SNE. *Journal of Machine Learning Research*, 9(86):2579–2605, 2008. URL <http://jmlr.org/papers/v9/vandermaaten08a.html>.

Appendix A. Centered Distance Based Results

A.1. The MDS Matrix is a Gram matrix

Assume centered \mathbf{X} (i.e. the column means of \mathbf{X} are zero). Then,

$$\begin{aligned}
 -\mathbf{HDH} &= -\left(\mathbf{I} - \frac{1}{n}\mathbf{1}\mathbf{1}^T\right)\mathbf{D}\left(\mathbf{I} - \frac{1}{n}\mathbf{1}\mathbf{1}^T\right) \\
 &= -\left(\mathbf{I} - \frac{1}{n}\mathbf{1}\mathbf{1}^T\right)\left(\tilde{\mathbf{D}}\mathbf{1}\mathbf{1}^T + \mathbf{1}\mathbf{1}^T\tilde{\mathbf{D}} - 2\mathbf{X}\mathbf{X}^T\right)\left(\mathbf{I} - \frac{1}{n}\mathbf{1}\mathbf{1}^T\right) \\
 &\dots \\
 &= 2\mathbf{X}\mathbf{X}^T - \frac{2}{n}\mathbf{X}\mathbf{X}^T\mathbf{1}\mathbf{1}^T - \frac{2}{n}\mathbf{1}\mathbf{1}^T\mathbf{X}\mathbf{X}^T + \frac{2}{n^2}\mathbf{1}\mathbf{1}^T\mathbf{X}\mathbf{X}^T\mathbf{1}\mathbf{1}^T \\
 &= 2\mathbf{X}\mathbf{X}^T
 \end{aligned}$$

A.2. $-\mathbf{HD}'\mathbf{H}$ is PSD

\mathbf{D}'_{ij} ^{0.5} (and \mathbf{D}'_{ij}) are valid distance metrics. We only need to show that $-\mathbf{D}'$ is CPSD, then, there exists an isometric Euclidean embedding [Khare \(2019\)](#); [Schoenberg \(1935\)](#). $-\mathbf{D}' = \log \frac{1}{1 + \|\mathbf{X}_i - \mathbf{X}_j\|^2}$. Note that the inner term is a kernel, hence is PSD. The log function preserves CPSD-ness ([Bhatia, 2007](#)).

Appendix B. A different interpretation of Equation (3)

If the negative samples coefficient of the second term of Equation (3) is absorbed into the logarithm, and the first term ignored, this implies that the edge probability is,

$$\begin{aligned}\mathbb{P}(\mathbf{A}_{ij} = 1) &= 1 - \left(1 - \frac{1}{1 + \|\mathbf{X}_i - \mathbf{X}_j\|^2}\right)^{1.5n_{\#}n_{-}/n} \\ &\approx \frac{1.5n_{\#}n_{-}}{n} \log \left(1 + \frac{1}{\|\mathbf{X}_i - \mathbf{X}_j\|^2 + \epsilon}\right).\end{aligned}$$

We further approximate this probability as the following based on empirical observations that it did not seem to affect the embeddings negatively,

$$\mathbb{P}(\mathbf{A}_{ij} = 1) \approx \frac{1.5n_{\#}n_{-}/n}{1 + \|\mathbf{X}_i - \mathbf{X}_j\|^2}.$$

Using this definition, we estimate the parameter of a Wishart distribution over the normalized graph Laplacian \mathbf{L} by moment matching (specifically such that the functional terms of the Wishart variance match the Bernoulli distribution's variances). This leads to the covariance estimate,

$$\mathbf{M}_{ij} = \frac{\mathbf{p}_{ij}}{\sum_a \mathbf{p}_{ia} \sum_b \mathbf{p}_{ib}},$$

where $\mathbf{p}_{ij} = \frac{1.5n_{\#}n_{-}/n}{1 + \|\mathbf{X}_i - \mathbf{X}_j\|^2}$. It's easy to see that this is PD. Plugging this in place of $\alpha\mathbf{M}$ into our model in Equation (4) leads to the embedding in ???. Note that the coefficient is around 0.01 when $n = 10k$, which might shed light into the choice for α that is most performant in Figure 4.

Appendix C. A Matrix-t Perspective

The density of the matrix-t distribution, with the column covariance set to \mathbf{I} is expressed as (Gupta and Nagar, 2018),

$$\log p(\mathbf{Y}|\Sigma) = -(\alpha + n/2) \log \left| \mathbf{I}_n + \frac{\beta}{2} \Sigma^{-1} \mathbf{Y} \mathbf{Y}^T \right| - \frac{d}{2} \log |\Sigma| + c.$$

Let $\mathbf{S} = \mathbf{\Gamma}^{-1}$ be an invertible estimator of $\mathbf{Y} \mathbf{Y}^T$. Note that,

$$\begin{aligned}\log \left| \mathbf{I}_n + \frac{\beta}{2} \Sigma^{-1} \mathbf{S} \right| &= \log \left| \frac{\beta}{2} \Sigma^{-1} \mathbf{S} \right| \left| \frac{2}{\beta} \mathbf{\Gamma} \Sigma + \mathbf{I}_n \right| \\ &= \log \left| \frac{2}{\beta} \mathbf{\Gamma} \Sigma + \mathbf{I}_n \right| - \log |\Sigma| + k.\end{aligned}$$

Therefore the density can be rewritten in terms of the precision matrix $\mathbf{\Gamma}$,

$$\log p(\mathbf{Y}|\Sigma) = \frac{2\alpha + n - d}{2} \log |\Sigma| - (\alpha + n/2) \log \left| \frac{2}{\beta} \mathbf{\Gamma} \Sigma + \mathbf{I}_n \right| + c.$$

For reference, the negative log-density of a matrix Cauchy distribution can be written as follows (adapted from),

$$\mathcal{L}_{t_1}(\Sigma) = \frac{d+n}{2} \log |I + \mathbf{L}\Sigma| - \frac{n}{2} \log |\Sigma| + c.$$

The first term of the CNE bound can also be approximated as,

$$\begin{aligned} & -\mathbb{E}_{ij \sim p} \log \left(\frac{w_{ij}(\mathbf{X})}{w_{ij}(\mathbf{X}) + 1} \right) \\ &= -\mathbb{E}_{ij \sim p} \log \left(\frac{1}{1 + \frac{1}{w_{ij}(\mathbf{X})}} \right) \\ &= -\mathbb{E}_{ij \sim p} \log \left(\frac{1}{2 + \|\mathbf{X}_i - \mathbf{X}_j\|^2} \right) \\ &= \mathbb{E}_{ij \sim p} \log (2 + \|\mathbf{X}_i - \mathbf{X}_j\|^2) \\ &\approx n^{-2} \sum_{ij} a_{ij} \log (1 + \|\mathbf{X}_i - \mathbf{X}_j\|^2) \\ &\leq \log(2 + n^{-2} \sum_{ij} a_{ij} \|\mathbf{X}_i - \mathbf{X}_j\|^2) \\ &= \log(1 + 2n^{-2} \text{tr}(\mathbf{L}\mathbf{X}\mathbf{X}^T + \mathbf{I})) \\ &\approx \log |\mathbf{I} + \mathbf{L}(\mathbf{X}\mathbf{X}^T + \mathbf{I})|. \end{aligned}$$

Following the methodology of Section 3.1 however leads to a very Laplacian-Eigenmaps-like solution. The regularisation term is paramount to the quality of embeddings obtained using such methods.

Appendix D. An Analysis of the Adjacency Probabilities

The generative probabilities of t-SNE, in some sense, model the probability with which an edge is the shortest edge on the entire distance graph, representing the shortest edge. The probability of this is proportional to $w_{ij}(\mathbf{X}) = \frac{1}{1 + \|\mathbf{X}_i - \mathbf{X}_j\|^2}$ (implied by the contrastive loss used in [Damrich et al. \(2022\)](#); this is also evident from the construction of the algorithm).

In this section, we assume that there’s a latent dataset described by a generative model $\mathbf{X} \rightarrow \mathbf{Y}$ that’s unobserved, but whose statistics then affect the data adjacency matrix \mathbf{A} through $\mathbf{Y} \rightarrow \mathbf{A}$, that is observed.

Assuming that a generative model for data \mathbf{Y} given latents \mathbf{X} exists, we show by simulation that $\mathbb{P}(\mathcal{A}_{ij}(\mathbf{Y}) = 1 | \mathbf{X}) = \mathbb{P} \left(\mathcal{I} \left[\|\mathbf{Y}_i - \mathbf{Y}_j\|^2 = \underset{k>l}{\text{argmin}} \|\mathbf{Y}_k - \mathbf{Y}_l\|^2 \right] = 1 | \mathbf{X} \right)$ cannot be proportional to the form assumed in t-SNE if a Gaussian process model,

$$\mathbf{Y} | \mathbf{X} \sim \mathcal{MN}(\mathbf{0}, \mathbf{X}\mathbf{X}^T + \sigma^2 \mathbf{I}, \mathbf{I}),$$

is assumed, but **can** be achieved by both matrix Cauchy distributions with a linear kernel and Gaussian processes with a kernel that is the sum of linear and smooth kernels. This is intuitive, as for these probabilities to decay to zero, in the Gaussian case, the kernel must be

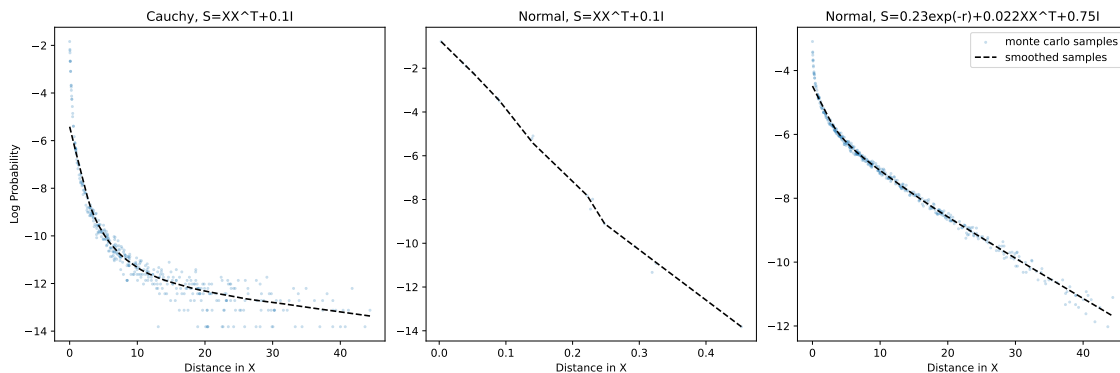


Figure 5: Monte-Carlo simulations showing the probability with which a distance $d_{ij}(\mathbf{Y})$ is the minimum throughout the entire distance matrix, plotted as a function of the Euclidean distance between the \mathbf{X} .

non-stationary. In the case of a matrix Cauchy distribution, this is due to its extreme-value properties.

Monte-Carlo simulations were done where a matrix Cauchy distribution (left on Figure 5) and a Gaussian process (right) with dot product kernels are used to generate high-dimensional data, and hence distance matrices between the high-dimensional data points. Then, the log probability that the ij^{th} element of the distance matrix is the smallest is computed and plotted against the Euclidean distances of the corresponding \mathbf{X} points. These show that using a Gaussian process with a linear kernel produces probabilities that are linear functions of the latent Euclidean distance. A matrix Cauchy prior on the other hand, induces proximity probabilities of the right shape.

As the linear kernel induces extremely small probabilities for larger distances in \mathbf{X} , we also use importance sampling to simulate tail probabilities and ensure that these behave linearly as a function of the distances in \mathbf{X} . For this, we need a full joint distribution of distances, which is approximated below.

Theorem 1 (Distribution of normal distances) *Assume that \mathbf{Y} is distributed as,*

$$\begin{bmatrix} \mathbf{Y}_i \\ \mathbf{Y}_j \end{bmatrix} \sim \mathcal{MN} \left(\mu, \begin{bmatrix} k_{ii} & k_{ij} \\ k_{ji} & k_{jj} \end{bmatrix}, \mathbf{I}_d \right).$$

Then, the following hold. Firstly, denoting $d_{ij}^2 = \|\mathbf{Y}_i - \mathbf{Y}_j\|^2$, the marginal distribution is given by,

$$d_{ij}^2 \sim \Gamma \left(k = \frac{d}{2}, \theta = 2(k_{ii} + k_{jj} - 2k_{ij}) \right).$$

*As a consequence, $\mathbb{E}(d_{ij}^2) = d * \tilde{k}_{ij}$ and $\mathbb{V}(d_{ij}^2) = 2d * \tilde{k}_{ij}^2$, where $\tilde{k}_{ij} = k_{ii} + k_{jj} - 2k_{ij}$. Additionally,*

$$\mathbb{C}(d_{ij}^2, d_{mn}^2) = 2d * (k_{im} + k_{jn} - k_{in} - k_{jm})^2.$$

This is a useful fact as the upper triangle of the distance matrix is approximately normal due to the central limit theorem with increasing d . Proved in Appendix E.

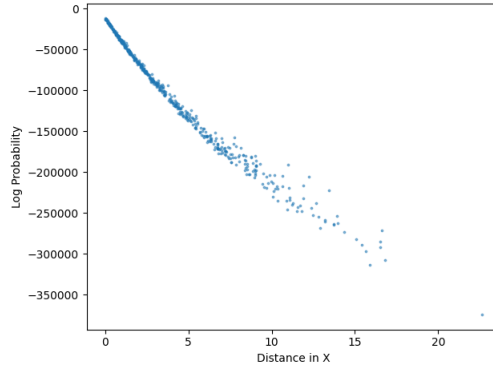


Figure 6: Illustration of $\mathbb{P}(\text{argmin}(d_{ij}^2) = ij)$ through importance sampling for a linear GP.

Results of this experiment are given in Figure 6, which confirms that a Gaussian process with a linear (dot product) kernel produces probabilities that are approximately linear functions of the latent distance, which are unlike the assumed tSNE adjacency probabilities.

Along different lines, we can think of the UMAP generative model as a model for adjacencies $\mathbf{A}_{ij} \sim \text{Bernoulli}(1/(1+\|\mathbf{X}_i - \mathbf{X}_j\|^2))$ as stated in ProbDR. Using just the mean the variance in Theorem 1, we can find the parameters of a covariance $\mathbf{S} = \alpha\mathbf{X}\mathbf{X}^T + \beta K_t(\mathbf{X}) + \gamma\mathbf{I}$, using a black-box optimiser such that the probability of a pair of points ij having a distance smaller than ϵ ,

$$\mathbb{P}(d_{ij}^2 < \epsilon) \approx \Phi\left(\frac{\epsilon - d\tilde{k}_{ij}}{\sqrt{2d\tilde{k}_{ij}}}\right),$$

with $\tilde{k}_{ij} = \alpha\|\mathbf{X}_i - \mathbf{X}_j\|^2 + 2\gamma + 2\beta(1 - 1/(1 + \|\mathbf{X}_i - \mathbf{X}_j\|^2))$, is as in UMAP. This results in the parameters $\alpha \approx 0.1, \beta \approx 0.3, \gamma \approx 0.6$, with the fit being near-perfect. However, we reason that this is quite a coarse approximation and a naive application of this covariance within ProbDR results in a mediocre embedding.

Appendix E. An Approximate Joint Distribution of Euclidean Distances

The first part of the theorem is given in Ravuri et al. 2023, reproduced below.

$$\begin{aligned} \forall k : d'_{ij} &\equiv y_i^k - y_j^k \sim \mathcal{N}(0, k_{ii} + k_{jj} - 2k_{ij}) \stackrel{d}{=} \sqrt{k_{ii} + k_{jj} - 2k_{ij}}Z \\ \Rightarrow d_{ij}^2 &\equiv \|\mathbf{Y}_i - \mathbf{Y}_j\|^2 = \sum_k (y_i^k - y_j^k)^2 \stackrel{d}{=} (k_{ii} + k_{jj} - 2k_{ij}) \sum_k Z_k^2 \\ &\stackrel{d}{=} (k_{ii} + k_{jj} - 2k_{ij})\chi_d^2 \\ &\stackrel{d}{=} \Gamma(k = d/2, \theta = 2(k_{ii} + k_{jj} - 2k_{ij})). \end{aligned}$$

The covariance between d_{ij}^2 and d_{mn}^2 can be computed as follows. Let,

$$d'_{ij} = \mathbf{Y}_{id} - \mathbf{Y}_{jd} \quad \text{and} \quad d'_{mn} = \mathbf{Y}_{md} - \mathbf{Y}_{nd}.$$

We can then derive some important moments as follows,

$$\mathbb{E}(d'_{ij}) = 0,$$

$$\mathbb{V}(d'_{ij}) = \mathbb{E}(d'^2_{ij}) = k_{ii} + k_{jj} - 2k_{ij},$$

$$\begin{aligned} \mathbb{C}(d'_{ij}, d'_{mn}) &= \mathbb{C}(Y_{id} - Y_{jd}, Y_{md} - Y_{nd}) \\ &= \mathbb{C}(Y_{id}, Y_{md}) - \mathbb{C}(Y_{id}, Y_{nd}) - \mathbb{C}(Y_{jd}, Y_{md}) + \mathbb{C}(Y_{jd}, Y_{nd}) \\ &= k_{im} + k_{jn} - k_{in} - k_{jm}, \end{aligned}$$

Then,

$$\begin{aligned} \mathbb{C}(d'^2_{ij}, d'^2_{mn}) &= \mathbb{C}\left(\sum_{d_1} (\mathbf{Y}_{id_1} - \mathbf{Y}_{jd_1})^2, \sum_{d_2} (\mathbf{Y}_{md_2} - \mathbf{Y}_{nd_2})^2\right) \\ &= \sum_{d_1} \sum_{d_2} \mathbb{C}((\mathbf{Y}_{id_1} - \mathbf{Y}_{jd_1})^2, (\mathbf{Y}_{md_2} - \mathbf{Y}_{nd_2})^2) && \text{linearity} \\ &= \sum_d \mathbb{C}(d'^2_{ij}, d'^2_{mn}) && \text{independence} \\ &= d * \mathbb{C}(d'^2_{ij}, d'^2_{mn}) \\ &= d * [\mathbb{E}[d'^2_{ij} d'^2_{mn}] - \mathbb{E}[d'^2_{ij}] \mathbb{E}[d'^2_{mn}]] \\ &= d * [\mathbb{E}(d'^2_{ij}) \mathbb{E}(d'^2_{mn}) + 2\mathbb{E}^2(d'_{ij} d'_{mn}) - \mathbb{E}[d'^2_{ij}] \mathbb{E}[d'^2_{mn}]] && \text{Isserlis' theorem} \\ &= 2d * \mathbb{E}^2(d'_{ij} d'_{mn}) \\ &= 2d * (k_{im} + k_{jn} - k_{in} - k_{jm})^2. \end{aligned}$$